The Deuteron Tensor Structure Function b_1

A Proposal to Jefferson Lab PAC-38.
(Update to LOI-11-003)

J.-P. Chen (co-spokesperson), P. Solvignon (co-spokesperson),
K. Allada, A. Camsonne, A. Deur, D. Gaskell,
C. Keith, S. Wood, J. Zhang
Thomas Jefferson National Accelerator Facility, Newport News, VA 23606

N. Kalantarians (co-spokesperson), O. Rondon (co-spokesperson)
Donal B. Day, Hovhannes Baghdasaryan, Zhihong Ye
University of Virginia, Charlottesville, VA 22903

K. Slifer[†](co-spokesperson), A. Atkins, T. Badman,
J. Calarco, J. Maxwell, S. Phillips, R. Zielinski
University of New Hampshire, Durham, NH 03861

D. Dutta
Mississippi State University, Mississippi State, MS 39762

G. Ron
Hebrew University of Jerusalem, Jerusalem

W. Bertozzi, S. Gilad,
A. Kelleher, V. Sulkosky
Massachusetts Institute of Technology, Cambridge, MA 02139

K. Adhikari
Old Dominion University, Norfolk, VA 23529

R. Gilman
Rutgers, The State University of New Jersey, Piscataway, NJ 08854

Seonho Choi, Hoyoung Kang, Hyekoo Kang, Yoomin Oh
Seoul National University, Seoul 151-747 Korea

[†]Contact person

Abstract

The EMC experiment revealed that only a small fraction of the nucleon spin is carried by quarks. Two decades later, the spin crisis remains an open issue. Quark orbital angular momentum is now considered to be one of the principal contributions in generating the nucleon spin, but a precise determination of this critical piece has remained elusive. The leading twist tensor structure function b_1 of spin-1 hadrons can provide new insight into this puzzle, since it is directly related to effects arising from orbital angular momentum, which differ from the case in a spin-1/2 target. For this reason, it provides a unique tool to study partonic effects, while also being sensitive to to coherent nuclear properties in the simplest nuclear system.

At low x, shielding/anti-shielding effects are expected to dominate b_1, while at moderate and high x, b_1 can provide a clean probe of novel QCD effects, such as hidden color due to 6-quark configuration. Since the deuteron wave function is relatively well known, any novel effects are expected to be readily observable. All available models predict a small or vanishing value of b_1 at moderate x. However, the first pioneer measurement of b_1 at HERMES revealed a crossover to large negative value in the region $0.2 < x < 0.5$.

At Jefferson Lab, we can precisely determine b_1 with an inclusive measurement of the tensor asymmetry A_{zz} in the region $0.29 < x < 0.50$, for $1.5 < Q^2 < 3.0$ GeV^2. This will provide access to the tensor quark polarization, and allow a test of the Close-Kumano sum rule which vanishes in the absence of tensor polarization in the quark sea. The JLab/UVa solid polarized deuterium target will be utilized along with the Hall C HMS/SHMS spectrometers, and an unpolarized 85 nA, 11 GeV incident beam during a 40.3 day measurement. Until now, tensor structure has been largely unexplored, so the study of these quantities holds the potential of initiating a new field of spin physics at Jefferson Lab.

Foreword

This proposal follows the letter of intent LOI-11-003 which was submitted to PAC 37. For convenience we reproduce the draft PAC report comments below. We note that we have changed the methodology to use Hall C's HMS/SHMS spectrometers. The Hall C option was explored in the appendix of our LOI but the uncertainty was found to be large due to the technique which depended on measuring absolute cross sections. We have modified this methodology to measure a ratio of cross sections, in which many of the unwanted systematic effects cancel

We have also expanded our discussion in Sec. 1.3 of the expected behaviour of $b_1(x)$, in order to strengthen the justification for measuring in the region $0.29 < x < 0.50$ where most models predict very small or vanishing values for $b_1(x)$, in contrast to the HERMES data.

LOI-11-003 *"The Deuteron Tensor Structure Function b1"*

Motivation*: The collaboration proposes to measure the deuteron tensor structure function b1 by measuring deep inelastic scattering from a tensor polarized deuterium. This structure function would be zero for a deuteron with constituents in a relative s-wave. The structure function b1 can be compared with conventional calculations of quark distribution functions convoluted with nucleon momentum distributions in the deuteron including the d-state admixture. Departures from such approach, as hinted at in pioneering data at HERMES, is conjectured to be sensitive to orbital angular momentum effects.*

Measurement and Feasibility*: The letter of intent proposes such experiment in Hall A using an 11 GeV beam and the SoLID spectrometer. The polarized target proposed is a ^{6}LiD target. The rates in the proposal only assume tensor polarizations that have been demonstrated previously. The projected precision on the tensor structure function using SoLID is compelling to improve on the HERMES measurement at small x and extend it into the large x region. The proposed measurement will allow to map out the qualitative behavior of b1, which will serve as a benchmark for theoretical interpretations. In the appendix to the LOI, a feasibility study has also been performed for a measurement in Hall C using the HMS/SHMS spectrometers. Given the projected precision obtained, such measurement using HMS/SHMS does not seem to be compelling at this stage.*

Issues*: The main issue is on the theoretical interpretation of such experiment. The authors are urged to consult some theorists to provide at least some qualitative behavior of b1 when making their physics case for a proposal.*

Recommendation*: The PAC encourages the submission of a fully developed proposal that addresses the issue raised above.*

Contents

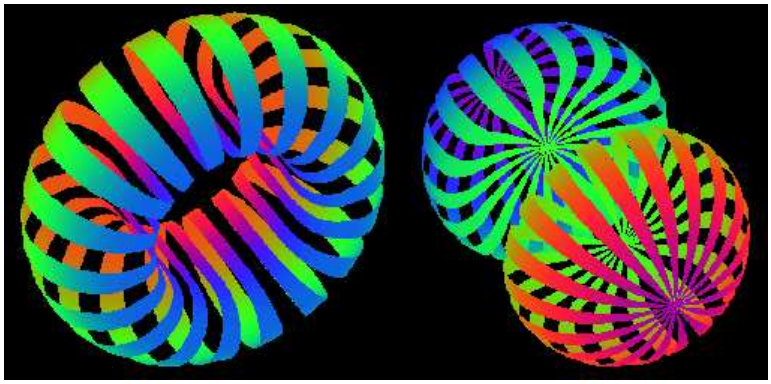

Figure 1: Nucleon densities of the deuteron in its two spin projections,$I_z = \pm 1$, and $I_z = 0$, respectively. *Reproduced from [2].*

1 Background and Motivation

The deuteron is the simplest nuclear system, and in many ways it is as important to understanding bound states in QCD as the hydrogen atom was to understanding bound systems in QED. Unlike it's atomic analogue, our understanding of the deuteron remains unsatisfying both experimentally and theoretically. A deeper understanding of the deuteron's tensor structure will help to clarify how the gross properties of the nucleus arise from the underlying partons. This provides novel information about nuclear structure, quark angular momentum, and the polarization of the quark sea that is not accessible in spin-1/2 targets.

A measurement of the tensor structure function b_1 is of considerable interest since it provides a clear measure of possible exotic effects in nuclei, i.e. the extent to which the nuclear ground state deviates from being a composite of nucleons only [1]. Jefferson Lab is the ideal place to investigate tensor structure in a deuteron target at intermediate and large x. We describe such a measurement in this proposal.

1.1 Tensor Structure of the Deuteron

When a spin 1 system such as the deuteron is subjected to a magnetic field along the z-axis, the Zeeman interaction gives rise to three magnetic sublevels $I_z = +1, 0, -1$ with population fractions p_+, p_-, p_0, respectively. These populations are described by both a vector polarization,

$$\begin{aligned} P_z &= \langle I_z/I \rangle \\ &= (p_+ - p_0) + (p_0 - p_+) = p_+ - p_- \end{aligned} \tag{1}$$

and a tensor polarization [3]:

$$\begin{aligned} P_{zz} &= \langle 3I_z^2 - I(I+1) \rangle / I^2 \\ &= (p_+ - p_0) - (p_0 - p_-) = 1 - 3p_0 \end{aligned} \tag{2}$$

which are subject to the overall normalization $p_+ + p_- + p_0 = 1$. In the case of deuteron spins in thermal equilibrium with the solid lattice, and neglecting the small quadrupole interaction [3], the tensor polarization is related to the vector polarization via:

$$P_{zz} = 2 - \sqrt{4 - 3P_z^2} \tag{3}$$

1.2 Deep Inelastic Scattering from Spin-1 Targets

Four independent helicity amplitudes are sufficient to describe virtual Compton scattering from a spin-1/2 target, after requiring parity and time reversal invariance. This number doubles for a spin-1 target, as the spin can be in three states (+, 0, -). This gives rise to a tensor structure which was first discussed for the deuteron for the real photon case by Pais [4], and later in the virtual photon case, by Frankfurt and Strikman [5]. Hoodbhoy, Jaffe and Manohar [6] introduced the notation which we now follow, whereby the tensor structure is described by the four functions b_1, b_2, b_3 and b_4. To summarize, the hadronic tensor can be decomposed as:

$$\begin{aligned} W_{\mu\nu} &= -F_1 g_{\mu\nu} + F_2 \frac{P_\mu P\nu}{\nu} \\ &\quad -b_1 r_{\mu\nu} + \frac{1}{6} b_2 (s_{\mu\nu} + t_{\mu\nu} + u_{\mu\nu}) \\ &\quad + \frac{1}{2} b_3 (s_{\mu\nu} - u_{\mu\nu}) + \frac{1}{2} b_4 (s_{\mu\nu} - t_{\mu\nu}) \\ &\quad + i \frac{g_1}{\nu} \epsilon_{\mu\nu\lambda\sigma} q^\lambda s^\sigma + i \frac{g_2}{\nu^2} \epsilon_{\mu\nu\lambda\sigma} q^\lambda (p \cdot q s^\sigma - s \cdot q p^\sigma) \end{aligned} \tag{4}$$

where the purely kinematic expressions $r_{\mu\nu}$, $s_{\mu\nu}$, $t_{\mu\nu}$ and $u_{\mu\nu}$ can be found in [6]. The terms are all proportional to the polarization of the target E. The spin-1 structure functions F_1, F_2, g_1 and g_2 have the same expressions and are measured the same way as for a spin-1/2 target. The spin-dependent structure functions b_1, b_2, b_3, b_4 are symmetric under $\mu \leftrightarrow \nu$ and $E \leftrightarrow E^*$ and therefore can be isolated from F_1 and g_1 by unpolarized beam scattering from a polarized spin-1 target.

1.2.1 Interpretation in the Operator Product Expansion

In the Operator Product Expansion (OPE) framework, the leading operators $O_V^{\mu_1 \cdots \mu_n}$ and $O_A^{\mu_1 \cdots \mu_n}$ in the expansion are twist two. For a spin-1 target, the matrix elements of the time-ordered product of two currents $T_{\mu\nu}$ have the following expressions:

$$\begin{aligned} < p, E | O_V^{\mu_1 \cdots \mu_n} | p, E > &= S[a_n p^{\mu_1} \ldots p^{\mu_n} + d_n (E^{*\mu_1} E^{\mu_2} - \frac{1}{3} p^{\mu_1} p^{\mu_2}) p^{\mu_3} \ldots p^{\mu_n}], \\ < p, E | O_A^{\mu_1 \cdots \mu_n} | p, E > &= S[r_n \epsilon^{\lambda\sigma\tau\mu_1} E^*_\lambda E_\sigma p_\tau p^{\mu_2}) \ldots p^{\mu_n}] \end{aligned} \tag{5}$$

The non-zero value of b_1 arises from the fact that, in a spin-1 target, the $\frac{1}{3} p^{\mu_1} p^{\mu_2}$ term doesn't cancel the tensor structure $E^{*\mu_1} E^{\mu_2}$. The coefficient d_n can be extracted from the comparison of

$T_{\mu\nu}$ expansion and the spin-1 target hadronic tensor Eq. 4 as follows:

$$\begin{aligned} b_1(\omega) &= \sum_{n=2,4,...}^{\infty} 2C_n^{(1)} d_n \omega^n, \\ b_2(\omega) &= \sum_{n=2,4,...}^{\infty} 4C_n^{(2)} d_n \omega^{n-1}, \end{aligned} \tag{6}$$

for $1 \leq |\omega| \leq \infty$ (where $\omega = 1/x$). A Callan-Gross-type relation exists for the two leading order tensor structure functions:

$$2xb_1 = b_2 \tag{7}$$

valid at lowest order of QCD, where $C_n^{(1)} = C_n^{(2)}$. At higher orders, Eq. 7 is violated.

Sum rules can be extracted from the moments of the tensor structure functions:

$$\begin{aligned} \int_0^1 x^{n-1}\, b_1(x)\, dx &= \frac{1}{2}\, C_n^{(1)}\, d_n, \\ \int_0^1 x^{n-2}\, b_2(x)\, dx &= C_n^{(2)}\, d_n, \end{aligned} \tag{8}$$

where n is even.

The OPE formalism is based on QCD and is target-independent. However, a target dependence is generated by Eq. 5, and spin-1 structure functions are subject to the same QCD corrections and their moments have the same anomalous dimensions as for a spin-1/2 target. In addition, the tensor structure functions should exhibit the same scaling behavior as F_1 and F_2, since they are generated from the same matrix element $O_V^{\mu_1 \cdots \mu_n}$.

We focus in this document on the leading twist structure function b_1. b_2 can be trivially determined from b_1, and b_3 and b_4 do not contribute at leading twist.

1.2.2 Interpretation in the Parton Model

In the infinite momentum frame[‡] of the parton model, the scattering of the virtual photon from a free quark with spin up (or down), which carries a momentum fraction x of the spin-m hadron, can be expressed through the hadronic tensor $W_{\mu\nu}^{(m)}$:

$$W_{\mu\nu}^{(1)} = \left(-\frac{1}{2} g_{\mu\nu} + \frac{x}{\nu} P_\mu P\nu \right) \Big(q_\uparrow^1(x) + q_\downarrow^1(x) \Big) + \frac{i\epsilon_{\mu\nu\lambda\sigma} q^\lambda s^\sigma}{2\nu} \Big(q_\uparrow^1(x) - q_\downarrow^1(x) \Big),$$

for a target of spin projection equal to 1 along the z-direction, and:

$$W_{\mu\nu}^{(0)} = \left(-\frac{1}{2} g_{\mu\nu} + \frac{x}{\nu} P_\mu P\nu \right) 2q_\uparrow^0(x) \tag{9}$$

[‡]All spins and momenta are along the z-axis.

for a target of spin projection equal to zero along the z-direction. The tensor structure functions b_1 and b_2 can be expressed from the comparison of $W^{(1)}_{\mu\nu} - W^{(0)}_{\mu\nu}$ with Eq. 4 as follows:

$$b_1(x) = \frac{1}{2}\Big(2q^0_\uparrow(x) - q^1_\uparrow(x) - q^1_\downarrow(x)\Big) \quad (10)$$

$$b_2(x) = 2xb_1(x) \quad (11)$$

where $q^m_\uparrow$ ($q^m_\downarrow$) represents the probability to find a quark with momentum fraction x and spin up (down) in a hadron which is in helicity state m. The tensor structure function b_1 depends only on the spin-averaged parton distributions[§]

$$q^1(x) = q^1_\uparrow(x) + q^1_\downarrow(x)$$
$$q^0(x) = q^0_\uparrow(x) + q^0_\downarrow(x) = 2q^0_\uparrow(x)$$

so

$$b_1(x) = \frac{q^0(x) - q^1(x)}{2} \quad (12)$$

Explicitly, b_1 measures the difference in partonic constituency in an $|m|$=1 target and an m=0 target. From this we see that while b_1 is expressed in terms of quark distributions, it interestingly depends also on the spin state of the nucleus as a whole.

1.2.3 First Measurement of $b_1(x)$ by the HERMES Collaboration

The HERMES collaboration made the first measurement [7, 8] of b_1 in 2005. The experiment explored the low x region of $0.001 < x < 0.45$ for $0.5 < Q^2 < 5$ GeV^2. An atomic beam source was used to generate a deuterium gas target with high tensor polarization. The HERA storage ring provided 27.6 GeV positrons incident on the internal gas target.

As displayed in Fig. 2, the tensor asymmetry A_{zz} was found to be non-zero at about the two sigma level, with an apparent zero crossing around $x = 0.3$. The tensor structure function b_1 exhibits a steep rise as $x \to 0$, which is qualitatively in agreement with the predictions of coherent double-scattering models. See for example Ref. [9]. The authors of Ref. [8] interpret the rapid rise at low x in terms of the same mechanism that leads to nuclear shadowing in unpolarized scattering.

As is often the case with a pioneer measurement, the precision of the results leaves some room for ambiguity. Despite the surprisingly large magnitude and interesting trend of the data, all points are roughly within two sigma from zero, which calls for a higher precision measurement. Another issue is that some of the HERMES momentum transfer values are low (see Fig. 3), so that quark structure functions may not be the correct language. The Q^2 variation in each x-bin is also quite wide ($\approx$10 GeV^2 for $x \sim 0.3$), which complicates the interpretation of this data, since several models predict significant Q^2-dependence of b_1. See for example Fig. 4.

[§]since, by parity, $q^m_\uparrow = q^m_\downarrow$

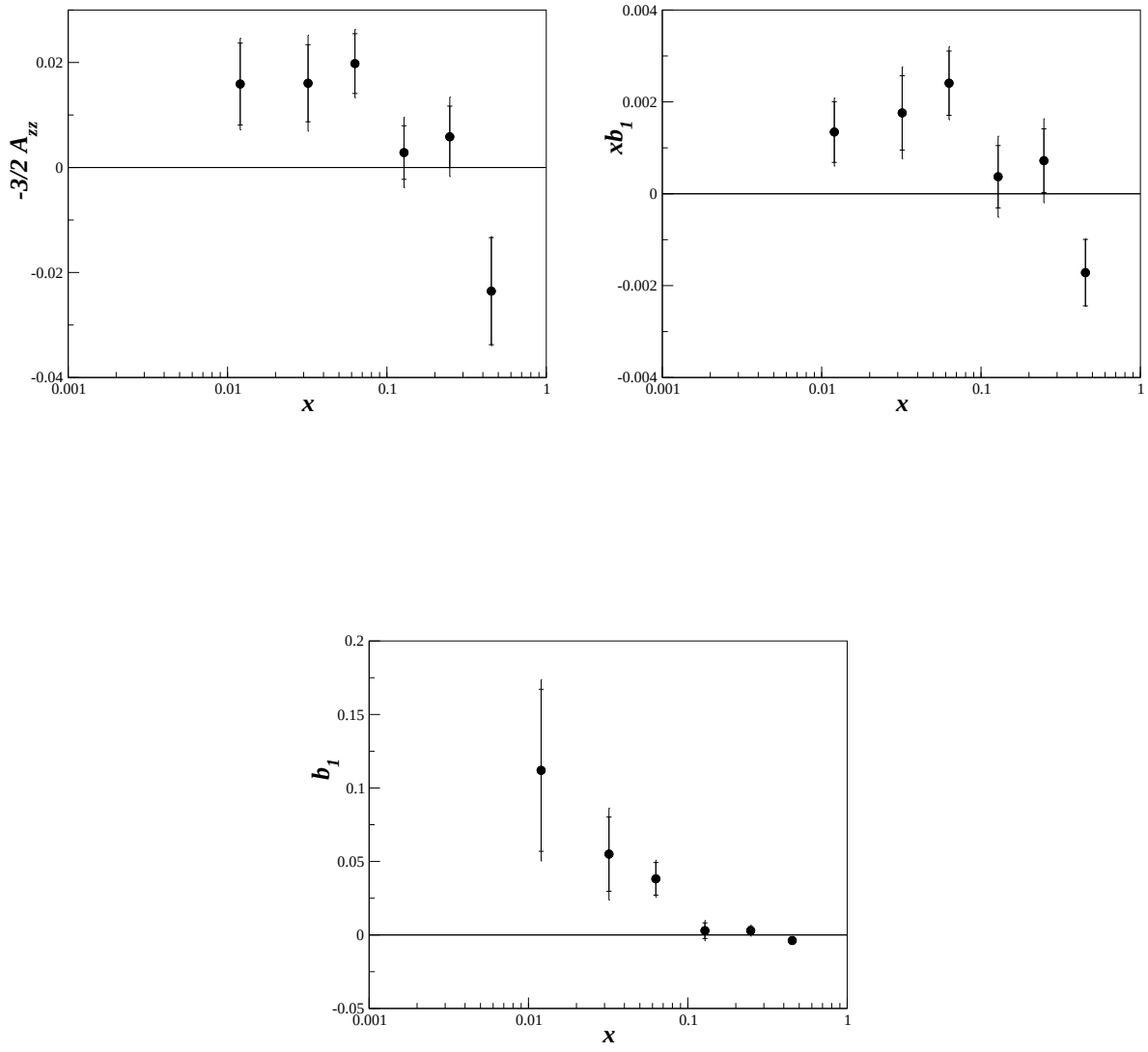

Figure 2: **Top**: HERMES [7] measurement of the inclusive tensor asymmetry $A_{zz}(x)$ and $xb_1(x)$ of the deuteron. **Bottom** : The tensor structure function $b_1(x)$ without x-weighting, which reveals a steep rise as $x \to 0$.

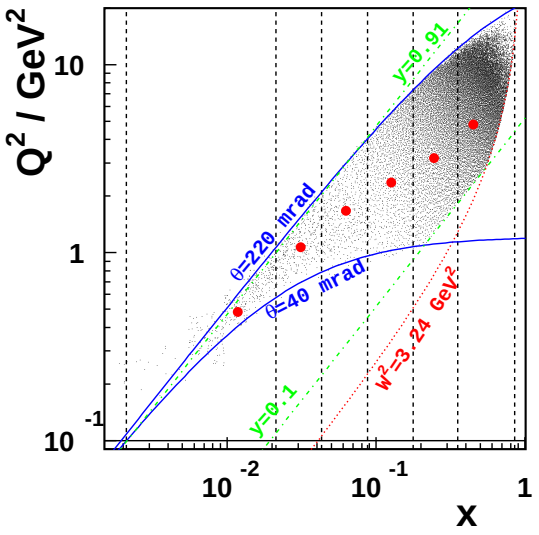

Figure 3: Kinematic coverage of the HERMES measurement. The dashed vertical lines indicate the borders of the bins in x, the dots their centers of gravity. The solid curves indicate the vertical acceptance of the spectrometer, defined by its aperture. In addition, the kinematic cuts imposed on the variables Q^2, y and W^2 are shown. *Reproduced from [7].*

1.3 Predictions for the Tensor Structure Function $b_1(x)$

The leading twist tensor structure function b_1 quantifies effects not present in the case of spin-1/2 hadrons. However, tensor effects only exist in nuclear targets, so the study of b_1 serves as a very interesting bridge between nucleon and nuclear physics. On the one hand, deep inelastic scattering (DIS), clearly probes partonic degrees of freedom, i.e. quarks, but on the other hand, b_1 depends solely on the deuteron (nuclear) spin state as seen in Eq. 11. We discuss now several predictions for the x dependence of b_1.

Hoodbhoy, Jaffe and Manohar

In Ref. [6], the authors evaluate the value of b_1 in three conventional scenarios for the deuteron constituents and their dynamics:

I. If the deuteron is composed of two spin-1/2 non-interacting nucleons at rest, then the eight helicity amplitudes characteristic of a spin-1 target are expressed in terms of the four helicity amplitudes of each spin-1/2 nucleons, and therefore the total number of independent amplitudes is reduced from eight to four. All structure functions of the deuteron are then the simple sum of the structure functions of the two nucleons, and the tensor structure functions vanish: $b_1 = b_2 = b_3 = b_4 = 0$.

II. If instead, the deuteron is composed of two spin-1/2 nucleons moving non-relativistically in a central potential, then the target motion modifies the helicity amplitudes. Using the

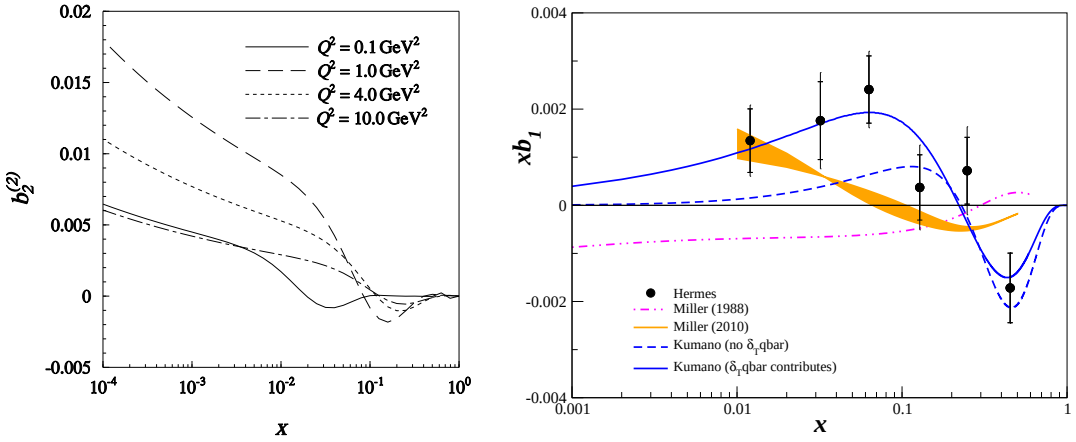

Figure 4: Theoretical predictions. **Left plot:** Double-scattering contribution to $b_2(x, Q^2)$ as a function of x [10]. Note the strong Q^2 dependence at low x. **Right plot:** HERMES results [8] compared to calculations from S. Kumano [11] and from the one-pion exchange effects of G. Miller [12, 13].

convolution formalism, it was found that the contribution of these moving nucleons to b_1 is small and is dominated by the lower component of the nucleon's Dirac wave function.

III. In the final scenario considered, the deuteron contains a D-state admixture. Because the proton and the neutron are moving in opposite directions, an additional term due to the $S - D$ interference appears in the convolution procedure. This extra contribution to b_1 is predicted to be even smaller than in the previous case.

All three scenarios predict a small or vanishing b_1. As a counter example for which b_1 could be significant, the authors consider a model of a massless relativistic quark with $j = 3/2$ moving in a central potential. In this calculation, a meson in the $j = 1$ state is formed from the coupling of a $P_{3/2}$ massless quark with a spin-1/2 spectator. This crude model predicts that $b_1(x)$ exhibits large negative values peaked around $x = 0.5$ [6]. Curiously, this behavior is possibly supported by the existing HERMES data (see Fig. 4), but there is only a single data point with large uncertainty in this region.

Miller

In 1988, Miller also examined the tensor structure function b_1 [12]. The basic mechanism is that the virtual photon hits an exchanged pion which is responsible for the binding of the deuteron. The calculation depends on the pion structure function which carries uncertainty. In this early calculation, the convention used by Miller for b_1 was different from that used in the HERMES results and in Ref. [11]. A recent update to this calculation [13], which uses a consistent convention, is shown in Fig. 4. Also the pion structure function from [14] was used. The spread of the curve originates from the parameter $A_s = (.9 \pm 0.3)$ which governs the strength of the sea in the pion. Miller's

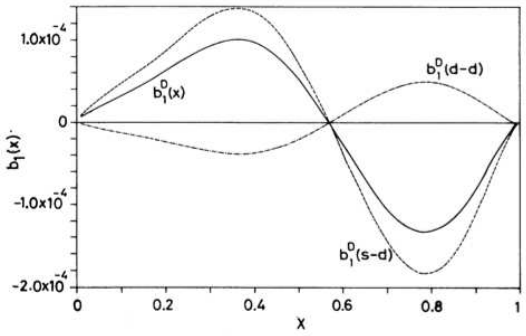

Figure 5: Prediction for $b_1^D(x)$ (solid curve) from Ref. [1], the S-D contribution to $b_1^D(x)$ (dashed curve), and the D-D contribution to $b_1^D(x)$ (dot-dashed curve). Note the vertical scale which would make the curve mostly indiscernible from zero in Fig. 4 (right). *Reproduced from Ref. [1].*

calculation, similar to other non-exotic models, is unable to reproduce the trend of the data at large x.

Khan and Hoodbhoy

Khan and Hoodbhoy [1] predict a small enhancement of b_1 in the region of $x \sim 0.3$, as seen in Fig. 5. Note however, that the absolute scale of this predicted b_1 is $\mathcal{O}(10^{-4})$, while the HERMES data implies that the scale is an order of magnitude larger than this.

Double-Scattering Effects

Using Vector Meson Dominance (VMD), the authors of Ref. [10] isolate the double-scattering contribution to b_1. The existence time of a vector meson can be described by the coherence length:

$$\lambda = \frac{Q^2}{Mx(M_v^2 + Q^2)} \tag{13}$$

which is the length over which the vector meson propagates during the time $\Delta t = 1/\Delta E$. Therefore, for multiple scattering to occur, a minimum coherence length of $\approx$ 1.7 fm (the inter-nucleon separation) is required. At $x > 0.3$, the coherence length is only about the size of the nucleon, so multiple scattering contributions are anticipated to be negligible. However, for $x \leq 0.1$, double-scattering should be significant in b_1 behaving as $(1-x)^{2\delta}/x^{1+2\delta}$, where δ is determined from the soft pomeron intercept $\alpha_P(t=0) = 1+\delta$. The authors predicted a significant enhancement of b_1 at low x ($\leq$ 0.01) due to the quadrupole deformation of the deuteron, which is qualitatively confirmed by the HERMES data. See Fig. 2.

Sargsian

M. Sargsian [15] recently calculated the tensor asymmetry A_{zz}. See Fig. 7.

Kumano's fit to $b_1(x)$ data

Recently, Kumano [11] estimated from an analysis of HERMES data [8] that a non-negligible tensor polarization of the sea is necessary to reproduce the trend of the data, as shown in Fig. 4. However, this conclusion has to be considered with caution due to the extended Q^2 coverage (Fig. 3), and large uncertainty of each HERMES data point.

1.4 The Close-Kumano Sum Rule

Following the formalism from the parton model in [6], Close and Kumano [16] related the tensor structure function b_1 to the electric quadrupole form factor of the spin-1 target through a sum rule:

$$\begin{aligned} \int_0^1 dx\, b_1(x) &= -\frac{5}{12M^2} \lim_{t\to 0}\, t\, F_Q(t) + \frac{1}{9}\Big(\delta Q + \delta\bar{Q}\Big)_s \\ &= \frac{1}{9}\Big(\delta Q + \delta\bar{Q}\Big)_s = 0 \end{aligned} \tag{14}$$

where $F_Q(t)$ is the electric quadrupole form factor of a spin-1 hadron at the momentum squared t. The Close Kumano (CK) sum rule is satisfied in the case of an unpolarized sea. The authors note that in nucleon-only models, the integral of b_1 is not sensitive to the tensor-polarization of the sea, and consequently the sum rule is always true, even when the deuteron is in a D-state.

In another approach, the authors of Ref. [1] calculated the first moment of $b_1(x)$ in a version of the convolution model that incorporates relativistic and binding energy corrections. They found a value of -6.65$\cdot 10^{-4}$, and emphasize that deviations from this will serve as a good signature of exotic effects in the deuteron wave function.

A truncated version of Eq. 14 was evaluated by the HERMES [7, 8] experiment and found to be:

$$\int_{0.0002}^{0.85} b_1(x)dx = 0.0105 \pm 0.0034 \pm 0.0035 \tag{15}$$

which possibly indicates a breaking of the Close-Kumano sum rule, and consequently a tensor-polarized quark sea. However, since the comparison is only at the two sigma level, more precise data is needed for a true test.

1.5 Interest from Theorists

During the preparation of this proposal, we contacted several theorists to gauge interest in a precision measurement of b_1. The response was uniformly positive. We provide some of their feedback for context.

It is known that b_1 is sensitive to dynamical aspects of constituents with angular momenta. Measurements of b_1 could open a new field of spin physics because this kind of spin physics has not

been explored anywhere else. Only experimental information came from the HERMES collaboration; however, their data are not accurate enough to find x dependence of b_1 especially at large x. It is an unique opportunity at JLab to develop this new field of spin physics.

S. Kumano (KEK)

I'm glad to hear that b_1 is not forgotten in all the excitement about other spin dependent effects.

R. Jaffe (MIT)

I am particularly interested in signatures of novel QCD effects in the deuteron. The tensor charge could be sensitive to hidden color (non-nucleonic) degrees of freedom at large x. It is also interesting that antishadowing in DIS in nuclei is not universal but depends on the quark flavor and spin. One can use counting rules from PQCD to predict the $x \to 1$ dependence of the tensor structure function.

S. Brodsky (SLAC)

I am certainly interested in the experimental development to find the novel QCD phenomena from the hidden color component of deuteron.

Chueng-Ryong Ji (NCSU)

2 The Proposed Experiment

We will measure the deuteron tensor asymmetry A_{zz} and extract the leading twist tensor structure function b_1 for $0.29 < x < 0.50$, $1.5 < Q^2 < 3.0$ GeV^2 and $W \geq 1.7$ GeV. Fig. 6 shows the kinematic coverage available at JLab utilizing an 11 GeV beam, and the Hall C HMS and SHMS spectrometers at forward angle.

The polarized LiD target is discussed in section 2.2. The vector polarization, packing fraction and dilution factor used in the estimate of the rates are 50%, 0.55 and 0.50 respectively. With an incident electron beam current of 85 nA, the expected deuteron luminosity is 2×10^{35} / cm^2·s^1. The momentum bite and the acceptance were assumed to be $\Delta P = \pm 8\%$ and $\Delta\Omega = 6.5$ msr for the HMS, and $\Delta P = ^{+20\%}_{-8\%}$ and $\Delta\Omega = 4.4$ msr for the SHMS. For the choice of the kinematics, special attention was taken onto the angular and momentum limits of the spectrometers: for the HMS, $10.5^\circ \leq \theta \leq 85^\circ$ and $1 \leq P_0 \leq 7.3$ GeV/c, and for the SHMS, $5.5^\circ \leq \theta \leq 40^\circ$ and $2 \leq P_0 \leq 11$ GeV/c. In addition, the opening angle between the spectrometers is physically constrained to be larger than 17.5°. The invariant mass W was constrained to $W \geq 1.7$ GeV for all settings. The projected uncertainties for A_{zz} and b_1 are summarized in Table 1 and displayed in Fig. 7. A total of 40.3 days of beam time is needed for production data.

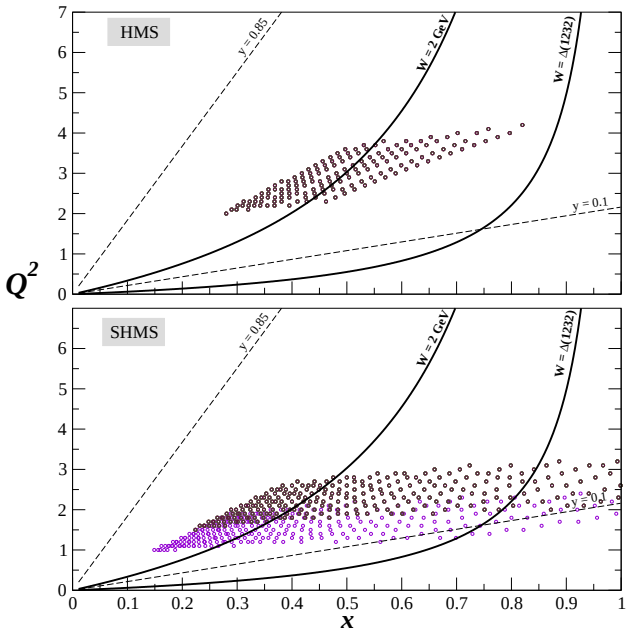

Figure 6: Kinematic coverage for 11 GeV beam in Hall C using the HMS and SHMS.

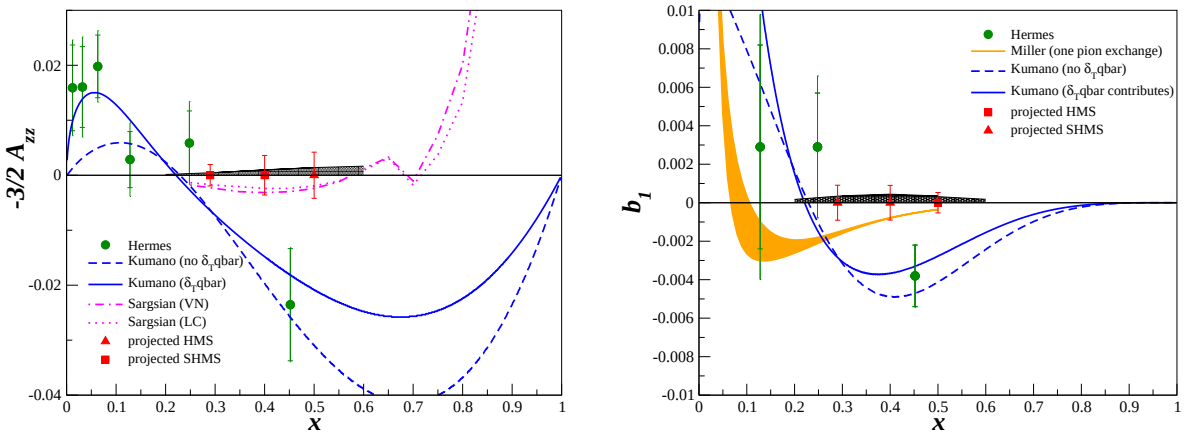

Figure 7: **Left:** Projected precision of the tensor asymmetry A_{zz} with 34 days of beam time. Also shown are the data from Hermes[8] and the calculation from Kumano [11] and Sargsian [15]. **Right:** Corresponding projected precision of the tensor structure function b_1. In addition, an updated calculation of Ref. [12] from Miller is shown [13]. The black band represents the systematic uncertainty.

	$\overline{x}$	$\overline{Q^2}$ (GeV^2)	$\overline{W}$ (GeV)	P_0 (GeV)	θ (deg.)	Rates (kHz)	A_{zz} $\times 10^{-2}$	δA_{zz}^{stat}	b_1 $\times 10^{-2}$	δb_1^{stat}	time (days)
HMS	0.50	3.0	2.0	7.95	10.6	0.06	1.4	0.28	-0.27	0.053	34
SHMS	0.29	1.5	2.2	8.37	7.3	0.65	0.43	0.13	-0.30	0.091	16
SHMS	0.40	2.2	2.1	8.20	9.0	0.17	0.99	0.24	-0.38	0.090	18

Table 1: Summary of the kinematics and physics rates using Hall C spectrometers.

2.1 Experimental Method

Following Ref. [6], we will measure the asymmetry A_{zz} by taking the difference of parallel and perpendicular polarized target cross sections, with an unpolarized¶ incident electron beam. For this configuration, it can be shown that:

$$\frac{\frac{d^2\sigma_\parallel}{d\Omega dE'} - \frac{d^2\sigma_\perp}{d\Omega dE'}}{\frac{d^2\sigma_\parallel}{d\Omega dE'} + 2\frac{d^2\sigma_\perp}{d\Omega dE'}} = -\frac{1}{2}(1 - \frac{3}{2}H^2)A_{zz}, \tag{16}$$

where $H^2 = (P+2)/3$, with P the deuteron vector polarization. The polarized cross sections $d^2\sigma_\parallel/d\Omega dE'$ and $d^2\sigma_\perp/d\Omega dE'$ can be extracted from data collected by scattering an unpolarized electron beam off a spin-1 target polarized longitudinally and perpendicularly to the electron beam direction. The tensor structure function b_1 can then be extracted from:

$$\frac{b_1}{F_1} = -\frac{3}{2}A_{zz} \tag{17}$$

From Eq. 16, the beam time needed to achieve an absolute uncertainty of δA_{zz} can be deduced as:

$$T = \frac{32}{9P_z^2}\frac{1}{R_D\ f\ (P_{zz}\ \delta A_{zz})^2} \tag{18}$$

where R_D is the deuteron rate, f the dilution factor and P_{zz} the tensor polarization.

Table 2 summarizes the systematic error estimate for the cross section measurement. The unpolarized structure function F_1 is needed to extract b_1 from A_{zz} using Eq. 17. This contributes an additional 5% relative, which raises the total systematic for b_1 to 11.8%.

2.1.1 Statistical error calculations of A_{zz} and b_1^d

Full details of the error calculation can be found in Ref. [17].

From section 6 of Ref. [6], we have:

¶Polarized beam is not required for this experiment, but would enable a simultaneous measurement of g_1. The tensor structure function b_1 can then be isolated by averaging the results of data with beam polarized parallel and anti-parallel. False asymmetries will be monitored by periodically flipping the target spin direction.

Source	(%)
Target Polarization	5.0
Radiative Corrections	5.0
Acceptance	6.0
Dilution/Packing fraction	5.0
Charge determination	1.0
VDC efficiency	1.0
PID detector efficiencies	$\leq$1
Software cut efficiency	$\leq$1
Energy	0.5
Total	10.7

Table 2: Major contributions to the cross section systematic.

	Time (hrs)	Number	Total Time (hrs)
Elastic calibration	48.0	1	48.0
Target dilution measurement	8.0	1	8.0
Configuration changes	16	4	64.0
Beam Energy measurement	2.0	2	4.0
BCM calibration	1.0	2	2.0
Target Annealing	2.5	4	10.0
Target Material Change	4.0	4	16.0

Table 3: Summary of the Overhead.

$$\frac{d\sigma_{\parallel}^{H}}{dxdy} = K\left[xF_1(x) + \left(\frac{2}{3} - H^2\right)xb_1(x)\right] \quad (19)$$

$$\frac{d\sigma_{\perp}^{H}}{dxdy} = K\left[xF_1(x) - \left(\frac{1}{3} - \frac{1}{2}H^2\right)xb_1(x)\right] \quad (20)$$

with $K = \frac{e^4 ME}{2\pi Q^4}[1 + (1-y)^2]$. For simplicity, we use $\sigma_{\parallel}$ for $\frac{d\sigma_{\parallel}^{H}}{dxdy}$ and $\sigma_{\perp}$ for $\frac{d\sigma_{\perp}^{H}}{dxdy}$.

We know that $H^2 = (P_z + 2)/3$, where P_z is the vector polarization of the target. And the tensor polarization P_{zz} is related to P_z via Eq. 3.

The tensor asymmetry A_{zz} depends on b_1 and F_1:

$$\frac{b_1}{F_1} = -\frac{3}{2}A_{zz} \quad (21)$$

Working with the equations of $\sigma_{\parallel}$ and $\sigma_{\perp}$, we can isolate A_{zz} to find:

$$\frac{\sigma_{\parallel} - \sigma_{\perp}}{\sigma_{\parallel} + 2\sigma_{\perp}} = \frac{1}{4}P_z A_{zz} \quad (22)$$

Note, that if the vector polarization in the parallel orientation $P_z^{\parallel}$ differs from the polarization in the perpendicular orientation $P_z^{\perp}$, then Eq. 22 is modified slightly to:

$$\frac{\sigma_{\parallel} - \sigma_{\perp}}{\kappa\sigma_{\parallel} + 2\sigma_{\perp}} = \frac{1}{4}P_z^{\parallel} A_{zz}$$

where $\kappa = P_z^{\perp}/P_z^{\parallel}$. We've assumed $\kappa = 1$ for rates calculations.

In order to calculate the statistical error on A_{zz} we start from:

$$(\delta A_{zz})^2 = \left(\frac{\delta A_{zz}}{\delta\sigma_{\parallel}}\right)^2 (\delta\sigma_{\parallel})^2 + \left(\frac{\delta A_{zz}}{\delta\sigma_{\perp}}\right)^2 (\delta\sigma_{\perp})^2 \quad (23)$$

and

$$\frac{\delta A_{zz}}{\delta\sigma_{\parallel}} = \frac{4}{P_z}\left[\frac{-(\sigma_{\parallel} - \sigma_{\perp})}{(\sigma_{\parallel} + 2\sigma_{\perp})^2} + \frac{1}{\sigma_{\parallel} + 2\sigma_{\perp}}\right]$$
$$= \frac{4}{P_z}\frac{3\sigma_{\perp}}{(\sigma_{\parallel} + 2\sigma_{\perp})^2}$$

$$\frac{\delta A_{zz}}{\delta\sigma_{\perp}} = \frac{4}{P_z}\left[\frac{-2(\sigma_{\parallel} - \sigma_{\perp})}{(\sigma_{\parallel} + 2\sigma_{\perp})^2} - \frac{1}{\sigma_{\parallel} + 2\sigma_{\perp}}\right]$$
$$= \frac{4}{P_z}\frac{-3\sigma_{\parallel}}{(\sigma_{\parallel} + 2\sigma_{\perp})^2}$$

to arrive at:

$$(\delta A_{zz})^2 = \left(\frac{4}{P_z}\right)^2 \left[\frac{9\sigma_\perp^2 \delta\sigma_\parallel^2 + 9\sigma_\parallel^2 \delta\sigma_\perp^2}{(\sigma_\parallel + 2\sigma_\perp)^4}\right] \tag{24}$$

The parallel and perpendicular cross sections have the same kinematical weight K. Since b_1 is very small compared to F_1 (or equivalently, A_{zz} is very small), we can make the assumption $\sigma_\parallel \approx \sigma_\perp \equiv \sigma$ and $\delta\sigma_\parallel \approx \delta\sigma_\perp \equiv \delta\sigma$.

$$(\delta A_{zz})^2 = \frac{9 \times 16}{P_z^2} \frac{2\sigma^2 \delta\sigma^2}{(3\sigma)^4} = \frac{32}{9P_z^2} \frac{\delta\sigma^2}{\sigma^2} \tag{25}$$

$$\delta A_{zz} = \frac{4\sqrt{2}}{3P_z} \frac{\delta\sigma}{\sigma} = \frac{4\sqrt{2}}{3P_z} \frac{1}{\sqrt{N}} \tag{26}$$

We determine N from the unpolarized cross section model [18], which then allows us to calculate the rates and the time.

$$N = \frac{32}{9} \frac{1}{P_z^2 (\delta A_{zz}^{meas})^2} \tag{27}$$

To get the rates as a function of the theoretical tensor asymmetry, we need to apply the dilution factors:

$$A_{zz}^{meas} = f P_{zz} A_{zz} \tag{28}$$

$$N = \frac{32}{9} \frac{1}{P_z^2 (f P_{zz} \delta A_{zz})^2} \tag{29}$$

We need $N/2$ events in parallel and perpendicular kinematics. If we had a pure deuterium target, the time need will be:

$$T = \frac{N}{R_D} = \frac{32}{9} \frac{1}{R_D P_z^2 (f P_{zz} \delta A_{zz})^2} \tag{30}$$

Now the deuterium rates are estimated from the unpolarized deuteron cross section model [18] σ_D:

$$R_D = \sigma_D \; dp \; d\Omega \; L = \sigma_D \; dp \; d\Omega \; \rho_D \; \frac{I}{e} \tag{31}$$

with $\rho_D = \rho_{LiD} \cdot f_{LiD} \cdot PF_{LiD}$, where f_{LiD} is the dilution and PF_{LiD} is the packing fraction.

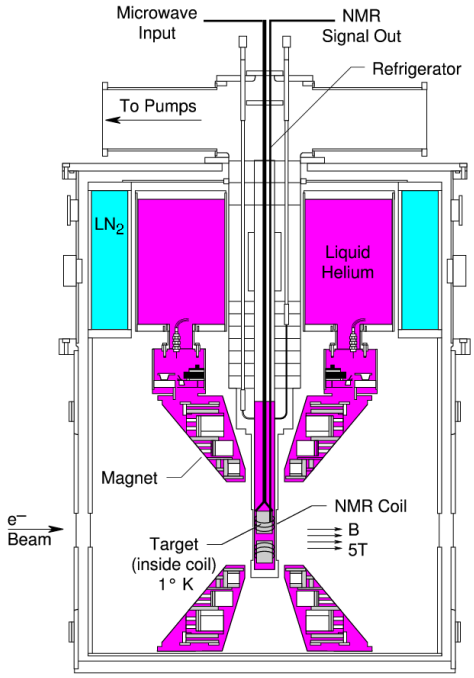

Figure 8: Cross section view of the JLab/UVa polarized target

2.1.2 Overhead

Table 3 summarizes the expected overhead, which sums to 6.3 days. In order to calibrate the target polarimetry, elastic scattering measurements will be performed at an incident energy of 2.2 GeV. Measurements of the dilution from the unpolarized materials contained in the target, and of the packing fraction due to the granular composition of the target material will be performed on a ^{6}Li target and carbon target. Target annealing will be performed approximately once per day, and target material changes will be performed about once a week. Configuration changes include rotation of the magnetic field of the target from parallel to perpendicular and vice versa.

2.2 Polarized Target

This experiment will require the installation of the JLab/UVa polarized target operated in longitudinal and also transverse mode. Transverse polarization requires operation of an upstream chicane to ensure proper transport through the target magnetic field. The target is typically operated with a specialized slow raster, and beamline instrumentation capable of characterizing the low current 50-100 nA beam. All of these requirements have been met previously in Hall C. The polarized target (see Fig. 8), has been successfully used in experiments E143, E155, and E155x at SLAC, and E93-026, E01-006 and E07-003 at JLab. The same target will be utilized in experiments E08-027 and E08-007 in late 2011. A similar target was used in Hall B for the EG1,EG4 and DVCS experiments, although Hall B does not at present have the facilities necessary to operate a transversely polarized target with an electron beam.

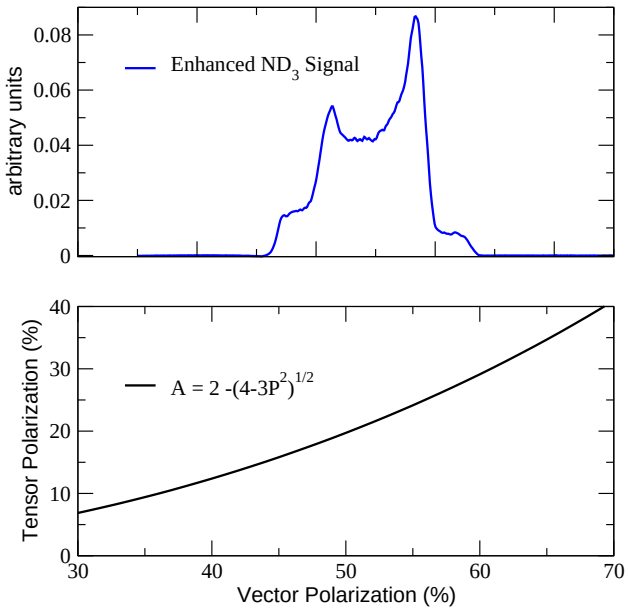

Figure 9: **Top**: NMR signal for ND_3 with a vector polarization of approximately 50% from the GeN experiment. **Bottom**: Relationship between vector and tensor polarization in equilibrium, and neglecting the small quadrupole interaction.

The target operates on the principle of Dynamic Nuclear Polarization, to enhance the low temperature (1 K), high magnetic field (5 T) polarization of solid materials by microwave pumping. The polarized target assembly contains several target cells of 3.0 cm length that can be selected individually by remote control to be located in the uniform field region of a superconducting Helmholtz pair. The permeable target cells are immersed in a vessel filled with liquid Helium and maintained at 1 K by use of a high power evaporation refrigerator. The coils have a 50° conical shaped aperture along the beam axis which allow for unobstructed forward scattering.

The target material is exposed to microwaves to drive the hyperfine transition which aligns the nucleon spins. The heating of the target by the beam causes a drop of a few percent in the polarization, and the polarization slowly decreases with time due to radiation damage. Most of the radiation damage can be repaired by periodically annealing the target, until the accumulated dose reached is greater than about 17×10^{15} e^-/cm^2, at which time the target material needs to be replaced.

2.2.1 Tensor Polarization

Eq. 3 allows calculation of a target's tensor polarization once the vector polarization has been determined from standard NMR techniques. Vector polarizations can be determined by analyzing NMR lineshapes as described in [19] with a typical 7% relative uncertainty, or by comparison of the NMR response to the known thermal equilibrium (TE) polarization with typical 5% uncertainty.

The DNP technique produces deuteron vector polarizations of up to 60% in ND_3 and 64% in LiD [20], which corresponds to tensor polarizations of approximately 30%. Tensor polarizations

of 22% have been achieved in previous experiments [3] using standard solid polarized ammonia targets.

At the University of Virginia and the University of New Hampshire, we are pursuing techniques to enhance the tensor polarization by directly stimulating transitions to/from the $M_s = 0$ state. The UVa group had some initial success in obtaining enhanced tensor polarizations via RF pumping, although the method was not pursued due to lack of need for tensor polarized targets at the time of the study. Another method entails simultaneously pumping the paramagnetic centers with two independent microwave frequencies, which requires careful isolation of the respective microwave cavities. The rates in this proposal assume only tensor polarizations that have been demonstrated previously.

3 Summary

We request 40.3 days of beam time in order to perform a precision measurement of b_1^d using a longitudinally polarized deuteron (LiD) target, together with the Hall C HMS and SHMS spectrometers. All existing theoretical predictions for b_1 in the region of interest predict small or vanishing values for b_1 at intermediate values of x, in contrast to the apparent large negative result of the only existing measurement from HERMES. Tensor structure measurements provide information not available from spin-1/2 targets. This measurement will help clarify the role quark orbital angular momentum plays in the nucleon spin, and open a new avenue of spin structure studies at Jefferson Lab.

References

[1] H. Khan and P. Hoodbhoy, Phys. Rev. **C44**, 1219 (1991).

[2] J. Carlson and R. Schiavilla, Rev. Mod. Phys. **70**, 743 (1998).

[3] W. Meyer *et al.*, Nucl. Instrum. Meth. **A244**, 574 (1986).

[4] A. Pais, Phys. Rev. Lett. **19**, 544 (1967).

[5] L. L. Frankfurt and M. I. Strikman, Nucl. Phys. **A405**, 557 (1983).

[6] P. Hoodbhoy, R. L. Jaffe, and A. Manohar, Nucl. Phys. **B312**, 571 (1989).

[7] C. Riedl, Ph. D thesis, DESY-THESIS-2005-027 (2005).

[8] A. Airapetian *et al.*, Phys. Rev. Lett. **95**, 242001 (2005).

[9] J. Edelmann, G. Piller, and W. Weise, Phys. Rev. **C57**, 3392 (1998).

[10] K. Bora and R. L. Jaffe, Phys. Rev. **D57**, 6906 (1998).

[11] S. Kumano, Phys. Rev. **D82**, 017501 (2010).

[12] G. A. Miller, In *Stanford 1989, Proceedings, Electronuclear physics with internal targets* 30-33. .

[13] G. A. Miller, private communication, to be published.

[14] P. J. Sutton, A. D. Martin, R. G. Roberts, and W. J. Stirling, Phys. Rev. **D45**, 2349 (1992).

[15] M. Sargsian, private communication, to be published.

[16] F. E. Close and S. Kumano, Phys. Rev. **D42**, 2377 (1990).

[17] P. Solvignon, b1 Technical note #06, (2011).

[18] A. D. Martin, W. J. Stirling, R. S. Thorne, and G. Watt, Eur. Phys. J. **C63**, 189 (2009).

[19] C. Dulya *et al.*, Nucl. Instrum. Meth. **A398**, 109 (1997).

[20] S. L. Bueltmann *et al.*, Nucl. Instrum. Meth. **A425**, 23 (1999).